Analytica Chimica Acta 1124 (2020) 137–145

Contents lists available at ScienceDirect

Analytica Chimica Acta

journal homepage: www.elsevier.com/locate/aca

Evaluation of exosome separation from human serum by frit-inlet asymmetrical flow field-flow fractionation and multiangle light scattering

Young Beom Kim , Joon Seon Yang , Gwang Bin Lee , Myeong Hee Moon *

Department of Chemistry, Yonsei University, 50 Yonsei-ro, Seoul, 03722, Republic of Korea

HIGHLIGHTS

- FlFFF-MALS was employed to investigate the isolation efficiency of serum exosomes.
- Exosomes can be separated from serum HDL and LDL by FlFFF with field programming.
- Ultrafiltration showed better retrieval with less volume than ultracentrifugation.
- Ultrafiltration with FlFFF-MALS can be a simple method for isolating serum exosomes.

GRAPHICAL ABSTRACT

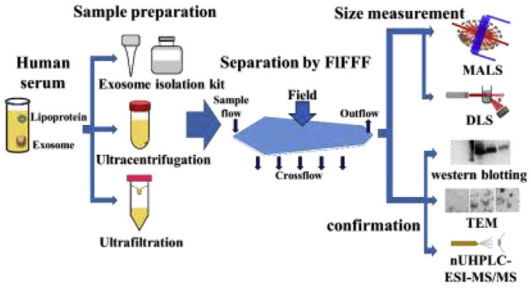

ARTICLE INFO

Article history:
Received 4 February 2020
Received in revised form
11 May 2020
Accepted 12 May 2020
Available online 16 May 2020

Keywords:
Frit-inlet asymmetrical flow field-flow fractionation
Exosome
Extracellular vesicle
Serum
Multiangle light scattering
nUHPLC-ESI-MS/MS

ABSTRACT

Exosomes are extracellular vesicles that mediate intercellular communication, immune response, and tumour metastasis. However, exosome isolation from the blood is complicated because their size and density are similar to those of blood lipoproteins. Here, we employed field programming frit-inlet asymmetrical flow field-flow fractionation (FIAF4) coupled with multiangle light scattering (MALS) for the effective separation of exosomes from free unbound proteins and lipoproteins present in serum samples using different pre-treatment methods, namely, a commercial exosome isolation kit, ultracentrifugation (UC), and a simple centrifugation followed by ultrafiltration (UF). Sizes of the eluted exosomes, as calculated by MALS signals, approximated well with the results of batch dynamic light scattering of the collected fractions and with the sizes of polystyrene particles. Exosome separation from lipoproteins was validated by western blotting with several markers of exosomes and lipoproteins, followed by proteomic analysis using nanoflow ultrahigh-performance liquid chromatography-electrospray ionisation-tandem mass spectrometry. UC requires relatively large amounts of serum samples (at least 2 mL) but is more efficient at removing lipoproteins. The UF method with a centrifugal concentrator (300 kDa) was found to be more effective in retrieving exosomes with low serum volumes (50 μL). Altogether, this study demonstrates the application of field programming FIAF4 for the isolation/purification of exosomes from proteins and lipoproteins in the serum.

1. Introduction

Exosomes are membrane-bound extracellular vesicles about thirty to several hundred nm in diameters. These are produced by

* Corresponding author.
E-mail address: mhmoon@yonsei.ac.kr (M.H. Moon).

https://doi.org/10.1016/j.aca.2020.05.031
0003-2670/

Abbreviations

FIAF4	frit-inlet asymmetrical flow field-flow fractionation
MALS	multiangle light scattering
UC	ultracentrifugation
UF	ultrafiltration
DLS	dynamic light scattering
SEC	size-exclusion chromatography
PEG	polyethylene glycol
HDL	high-density lipoprotein
LDL	low-density lipoprotein
VLDL	very low-density lipoprotein
FlFFF	flow field-flow fractionation
TEM	transmission electron microscopy
nUHPLC-ESI-MS/MS	nanoflow ultrahigh-performance liquid chromatography-electrospray ionisation-tandem mass spectrometry
CID	collision-induced dissociation

the inward budding of endosomes inside the cell, and are subsequently secreted out [1–3]. As exosomes contain proteins, RNA, lipids, and metabolites of the original cell, they are thought to be involved in physiological and pathological processes, including immune response, intercellular communication, and tumour initiation and metastasis [4–6]. Therefore, exosomes have garnered attention for their potential role in immune regulation and for the discovery of biomarkers for the diagnosis of cancers and other diseases [7]. However, the isolation and purification of exosomes is challenging, owing to their diversity in body fluids.

Isolation of exosomes can be carried out with ultracentrifugation (UC) [8], size-exclusion chromatography (SEC) [9], polyethylene glycol (PEG) precipitation [10], immunoaffinity capture [11,12], and density-gradient centrifugation using sucrose [12,13]. UC is commonly employed for exosome isolation but requires considerable amounts of samples, while its efficiency in terms of time and purity is relatively low [14,15]. SEC fails to exclude unwanted interactions of exosomes with the stationary phase, thereby resulting in exosome aggregation or loss. While precipitation with PEG is an efficient strategy with cell culture supernatant [10], the extension of this technique to blood plasma or serum has not been investigated. Density-gradient centrifugation of serum samples is relatively fast, but the yield is low and the resulting exosome fraction may be damaged due to high osmotic pressure or might contain several proteins and other vesicles such as lipoproteins. Immunoaffinity-based methods may increase the purity of the isolated exosomes but suffer from low yield, as the specific capture markers used may not be recognised by all exosome vesicles [16]. The product yield of most of these methods is relatively low. Moreover, it is difficult to completely isolate exosomes from blood samples owing to the presence of lipoproteins [17,18]. The analysis of lipids in exosomes from the blood system requires successful separation of exosomes from lipoproteins. Lipoproteins are classified into the following: high-density lipoprotein (HDL, 5–15 nm), low-density lipoprotein (LDL, 18–28 nm), and very low-density lipoprotein (VLDL, 30–80 nm). The combined use of SEC and UC [19] or affinity chromatography [20] may facilitate the separation of exosomes from lipoproteins but could be time consuming and result in low yield. In addition, one may still encounter unwanted interactions between vesicles and packing materials.

Flow field-flow fractionation (FlFFF) may serve as an alternative for the separation of exosomes by avoiding any physical interaction with packing materials. FlFFF is an elution-based method capable of separating macromolecules or particles based on their sizes (in the range of nanometres to microns) [21–23]. In FlFFF, particle separation is achieved based on the differences in the diffusion of sample components. This may facilitate the size-based separation of macromolecular species in an increasing order of hydrodynamic diameter [24]. As separation in a typical FlFFF system is achieved using a thin and unobstructed channel following interaction of two flow streams, a crossflow to inhibit the migration of sample components and a migration flow to drive sample species toward the end of the channel may prevent unwanted interactions between sample and packing materials as observed with chromatographic systems. The use of an aqueous solution, including a biological buffer as a carrier liquid for separation, has extended the application of FlFFF to different biological materials such as proteins, ribosomal subunits [25], virus-like particles [26], lipoproteins [27,28], subcellular organelles [29], and cells [30,31]. In particular, FlFFF demonstrated the capability to separate exosomes isolated from urine samples of patients with prostate cancer [32] and from other cellular origins [33,34]. However, separation of exosomes from the serum is still a challenge, owing to their similarity in size with lipoproteins.

In this study, we introduced an analytical method for the isolation of exosomes from a small amount of human serum sample using FlFFF and multiangle light scattering (MALS). We employed the crossflow programming in a frit-inlet asymmetrical FlFFF (FIAF4) channel system for separating exosomes with minimum contamination of lipoproteins along with an improved MALS-based exosome detection. Since sample relaxation in FI-AF4 channel can be achieved by hydrodynamically without focusing/relaxation procedure, the possibility of sample adhesion to channel membrane and their aggregation can be minimized. The effects of using UC, ultrafiltration (UF), and an exosome isolation kit on the isolation of exosomes prior to FlFFF separation were studied. The eluted fractions collected during FlFFF runs were analysed with transmission electron microscopy (TEM), western blotting, dynamic light scattering (DLS), and proteomics using nanoflow ultrahigh-performance liquid chromatography-electrospray ionisation-tandem mass spectrometry (nUHPLC-ESI-MS/MS).

2. Materials and methods

2.1. Materials and reagents

Human serum standard (sterile-filtered male AB plasma of USA origin), sodium chloride, sodium phosphate dibasic heptahydrate, potassium chloride, potassium phosphate monobasic, HDL standard from human plasma, rabbit anti-apolipoprotein B antibody, sodium dodecyl sulfate (SDS), and sodium azide (NaN_3) were purchased from Sigma-Aldrich (St. Louis, MO, USA). LDL and VLDL standards from human plasma were obtained from Merck Millipore (Darmstadt, Germany). Polystyrene standards with nominal diameters (22, 46, 102, and 203 nm) were supplied by Thermo Fisher Scientific (Waltham, MA, USA). Primary antibodies (mouse anti-ALIX, rabbit anti-CD9, rabbit anti-heat shock protein 70 [HSP70], and rabbit anti-apolipoprotein A1) and secondary antibodies (goat anti-rabbit IgG H&L [horse radish peroxide, HRP] and rabbit anti-mouse IgG H&L [HRP]) were purchased from Abcam Plc. (Cambridge, UK). Primary rabbit anti-TSG101 was procured from System Bioscience Inc. (Mountain View, CA, USA). For detection of chemiluminescence in western blotting, EZ-Western Lumi Femto Kit was purchased from DoGenBio Co. Ltd. (Seoul, Korea).

2.2. Sample preparation for exosome isolation

A human serum sample stored at −80 °C was thawed at 4 °C and treated with the following three preparation methods prior to the FlFFF separation of serum exosome: 1) an exosome isolation kit, 2) UC at 120,000×*g*, and 3) UF using two different centrifugal concentrators (MWCO 100 and 300 kDa). For the isolation of exosomes with the kit, the serum sample (500 μL) was treated with ExoLutE® Exosome Isolation Kit from Rosetta Exosome Inc. (Seoul, Korea) as per the manufacturer's protocol to remove lipoproteins. The resulting purified sample was directly used for FlFFF. During UC, 2 mL of the serum sample was first centrifuged at 1,000×*g* for 5 min to remove cell debris, and the supernatant was centrifuged at 10,000×*g* for 10 min to remove microvesicles. The supernatant liquid was transferred to a polycarbonate ultracentrifuge tube procured from Beckman Coulter Inc. (Brea, CA, USA) and centrifuged at 120,000×*g* for 2 h using Optima XE-100 Ultracentrifuge (Beckman Coulter) under 4 °C. The supernatant was removed and the exosome pellet was resuspended in 100 μL of 0.01 M phosphate-buffered saline (PBS), vortexed for 10 min, and stored at 4 °C for FlFFF analysis. For UF, the serum sample was subjected to a two-step centrifugation step (described above) to remove cell debris and microvesicles. The resulting supernatant was transferred to a Vivaspin® centrifugal concentrator (cut-off MW of 100,000 or 300,000 Da; Sartorius AG, Goettingen, Germany) and centrifuged at 5,000×*g* for 30 min under 4 °C. The retentate was collected and stored at 4 °C for FlFFF analysis.

2.3. FlFFF-UV-MALS of serum exosome extracts

The FlFFF system used in this study was an FIAF4 channel modified from a model LC channel (27.5 cm, length)—from Wyatt Technology Europe GmbH (Dernbach, Germany)—in our laboratory by replacing the depletion wall inlay with a new polycarbonate inlay, which was embedded with a ceramic inlet frit (35 mm × 18 mm × 7 mm). The channel spacer was prepared from a 350 μm thick Teflon sheet cut as per the channel's dimensions, 26.6 cm of tip-to-tip length and a trapezoidal decrease in the channel breadth (2.2 cm for the inlet and 0.6 cm for the outlet breadth). A regenerated cellulose membrane (MWCO 10 kDa; Wyatt Technology Europe GmbH) was used as the channel membrane. Two different carrier solutions were prepared using ultrapure water (>18 MΩ cm) as follows: 0.05% SDS solution added to 0.02% NaN_3 as a bactericide for polystyrene separation, and 0.01 M PBS solution was used for the separation of serum samples. All carrier solutions were filtered with a Durapore® hydrophilic polyvinylidene fluoride membrane filter (0.1 μm pore size; Merck Millipore) and degassed for 1 h prior to use. For sample injection, a model 7725i loop injector with a 100 μL sample loop (Rheodyne, Cotati, CA, USA) was used with a SP930D high-performance liquid chromatography (HPLC) pump from Young-Lin Instruments (Seoul, Korea). The frit flow was delivered to the frit-inlet by a model 1260 Infinity HPLC pump (Agilent Technologies, Palo Alto, CA, USA). The frit flow rate, outflow rate, and crossflow rate were controlled by Eclipse Separation System for AF4 (Wyatt Technology). Flow rates for sample injection and outflow were fixed at 0.08 and 0.48 mL/min, respectively. Field programming was applied to FIAF4 channel with a linear field decay pattern, wherein the crossflow rate was linearly reduced. The crossflow rate began with 1.5 mL/min for 3 min of the initial delay and then linearly decreased from 1.5 to 1.0 mL/min for 2 min to 0.9 mL/min for 14 min, 0.5 mL/min for 5 min, 0.1 mL/min for 10 min, and finally to 0.02 mL/min for 3 min; the flow was then maintained at 0.02 mL/min until the end of the run. Eluting sample components were monitored at a wavelength of 254 nm for polystyrene (PS) latex standards and 280 nm for serum samples using a series of detectors, including a model UV730D UV/Vis detector from Young-Lin and DAWN HELEOS II MALS detector at a wavelength of 658 nm from Wyatt Technology Europe GmbH. The detector signals were recorded using ASTRA software (Wyatt), which was used for the size calculation of exosomes using both Zimm and Sphere approximations. Fractions collected during FIAF4 separation were stored at 4 °C for further analysis with TEM, western blotting, and nUHPLC-ESI-MS/MS.

2.4. TEM analysis

Five UF fractions were collected during five consecutive runs of FlFFF at an interval of 5.0–8.5, 12.0–18.0, 20.0–28.0, 28.0–34.0, and 34.0–42.0 min. Each fraction was concentrated to ~100 μL using an Amicon Ultra-15 Centrifugal filter (30 kDa cutoff; Merck Millipore). Microscopic examination of particulate species from serum fractions was performed after negative staining using a model JEM-1011 transmission electron microscope (JEOL Ltd., Tokyo, Japan). In brief, 10 μL of each enriched fraction was placed on a Formvar coated with carbon layer on 300-mesh copper grids from Ted Pella Inc. (Redding, CA, USA) and fixed for 1 min. Water droplets were removed using filter paper. Each specimen was negatively stained with 2 μL of a 2% uranyl acetate solution (Ted Pella Inc.) for 15 s before it was completely dried. The excess of uranyl acetate was washed, and the specimen was dried for 30 min.

2.5. Western blotting

Fractions collected during FlFFF runs were confirmed by western blotting. Each fraction was concentrated to about 200 μL using an Amicon Ultra-15 Centrifugal filter. The enriched solution was lysed using an ultrasonic tip sonicator (Cole-Parmer Ltd., Vernon Hills, IL, USA) for 5 min at a pulse duration of 10 s at 2 s intervals for the Bradford assay. Based on the measured amount of protein in each fraction, sample solutions equivalent to 10 μg of protein were mixed with an SDS-polyacrylamide gel electrophoresis (PAGE) loading buffer (Curebio Ltd., Seoul, Korea) and heated for protein denaturation at 90 °C for 5 min. Electrophoresis was performed using a 10% polyacrylamide gel on a Mini-PROTEAN Tetra Cell System (Bio-Rad Laboratories Inc., Hercules, CA, USA) at an applied voltage of 80 V for the stacking gel and 120 V for electrophoresis. The separated proteins were transferred onto polyvinylidene difluoride (PVDF) membranes (0.45 μm pore size; Bio-Rad Laboratories Inc.) at 100 V for 90 min. The membranes were blocked for 1 h using a blocking solution (5% [w/v] skim milk in Tris-buffered saline plus Tween [TBS-T]) and then incubated with primary antibodies for 1 h at room temperature, followed by washing with TBS-T for 30 min. The membranes were incubated with secondary antibodies at room temperature for 1 h and then washed for 30 min. Detection of stained bands was carried out on an LAS-4000 detector (GE Healthcare, Little Chalfont, UK).

2.6. Particle size measurement by DLS

The average particle diameter of particles in the FlFFF fraction was measured by batch DLS using ELSZ-1000 Particle Size Analyzer (Otsuka Electronics, Hirakata, Japan). For the batch DLS measurement, each collected fraction was accumulated during five consecutive FlFFF runs. Before DLS measurement, each collected fraction was concentrated to about 3 mL using Amicon Ultra-15 Centrifugal filter (30 kDa cutoff). The concentration of each fraction was adjusted to avoid any saturation of signal intensity.

2.7. In-solution digestion of FlFFF fractions

Proteomic analysis was performed for each fraction to confirm the presence of exosomes. An aliquot equivalent to 50 μg of protein from the FlFFF fraction enriched after sonication was aliquoted and suspended in 0.01 M PBS. The mixture was treated with 8 M urea containing 10 mM dithiothreitol (DTT) and incubated at 37 °C for 2 h. Alkylation of thiol groups was performed with the addition of iodoacetamide to the mixture at a final concentration of 20 mM at 0 °C for 2 h in the dark. After alkylation, extra iodoacetamide was removed using an excess of cysteine (40 ×), while the remaining mixture was diluted with 0.01 M PBS to obtain a final urea concentration of 1.0 M. The mixture was treated with proteomic-grade trypsin at a ratio of 1:50 (protein:trypsin) and incubated at 37 °C for 24 h. After digestion, the mixture was desalted using Oasis HLB cartridge from Waters (Milford, MA, USA) and dried with a vacuum centrifuge. The dried powder was re-suspended in an aqueous solution containing 2% acetonitrile (CH_3CN) with 0.1% formic acid at a concentration of 1 μg/μL for nUHPLC-ESI-MS/MS analysis.

2.8. Proteomic analysis

Proteomic analysis of exosome fractions was carried out using a Dionex Ultimate 3000 RSLCnano liquid chromatography (LC) system coupled to a Q Exactive Hybrid Quadrupole-Orbitrap mass spectrometer (Thermo Fischer Scientific, San Jose, CA, USA). An analytical column (15 cm × 100 μm i.d.) was prepared in a capillary by packing 3.5 μm-130 Å XBridge Peptide BEH (ethylene-bridged hybrid) C18 particles unpacked from a BEH column (Waters), as previously described [35]. A home-made trap column was prepared in a 200 μm i.d. capillary tube for 3 cm by packing 3 μm-200 Å Magic C18AQ particles obtained from Michrom Bioresources Inc. (Auburn, CA, USA) [35]. Mobile phase solutions for binary-gradient elution were 98:2 (v/v) H_2O:CH_3CN for A and 20:80 (v/v) H_2O:CH_3CN for B. Both solutions were mixed with 0.1% formic acid. Gradient elution was initiated by ramping the mobile phase B to 10% for 1 min, to 30% B for 34 min, further to 80% B for 2 min, and was then maintained for 5 min. Then it was resumed with 1% B for 2 min and re-conditioned for the next run for 6 min. Column flow rate was adjusted to 200 nL/min by splitting the pump flow (4 μL/min) using a pressure capillary tube (20 μm i.d) connected to a 10-port valve. The experimental conditions for MS were as follows: +2.5 kV for ESI, m/z 300–1800 for the precursor scan, and 35.0% normalised collision energy for collision-induced dissociation (CID) experiments. Detection parameters were 10 s for repeat duration, 180 s for exclusion duration, and ±2.50 Da for mass exclusion. MS/MS spectra were analysed with Proteome Discover Software (version 1.4) from Fisher Scientific against nrNCBI human proteome database. The mass tolerance values were 1.0 Da for precursor ions and 0.8 Da for product ions with ΔCn score (0.1); minimum cross-correlation (Xcorr) values (2.4, 2.7, and 3.7 for +1, +2, and +3 charged ions, respectively), and the false discovery rate (0.01). Exosomal proteins of each fraction were compared with ExoCarta database (http://exocarta.org/).

3. Results and discussion

3.1. FlFFF-MALS separation of serum exosomes treated using UC and UF methods

The size fractionation capability of a relatively thick FIAF4 channel (w = 350 μm) with or without field programming was evaluated by separating lipoprotein standards. Fig. 1 shows the comparison of the separation of different lipoprotein standards using isocratic field strength, a fixed crossflow rate ($\dot{V}_c$) of 1.0 mL/min (top), and crossflow programming (bottom) with an initial $\dot{V}_c$ of 1.5 mL/min followed by a linear decay. Both runs were performed at a fixed sample flow ($\dot{V}_s$) to outflow ($\dot{V}_{out}$) rate of 0.08/0.48 (in mL/min) and a frit flow rate ($\dot{V}_f$) that was adjusted to $\dot{V}_f = \dot{V}_c + \dot{V}_{out} - \dot{V}_s$. Given the use of a thicker channel as compared with a typical FlFFF channel (w ≤ 250 μm) for lipoprotein separation, the retention time of lipoprotein standards at a constant field strength of $\dot{V}_c$ = 1.0 mL/min was very long and resulted in broad peaks. However, the application of crossflow programming could successfully resolve lipoprotein standards (HDL, LDL, and VLDL), although the peak of VLDL was still broad. The thicker channel used herein was to increase the level of retention which can eventually improve the separation resolution in FlFFF without incorporating a high field strength. Increasing the channel thickness can be helpful to resolve lipoprotein particles from lower size limit of exosomes but necessitates a field decay program with a high initial field strength to facilitate the elution of long retaining EVs, including exosomes.

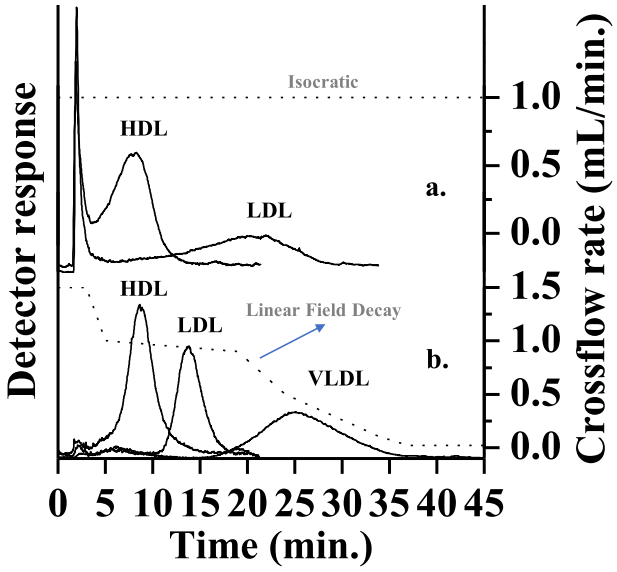

Fig. 1. Fractograms of lipoprotein standards by FIAF4 with (a) a constant field strength and (b) field programming. Sample flow rate ($\dot{V}_s$) = 0.08 mL/min, outflow rate ($\dot{V}_{out}$) = 0.48 mL/min, and w = 350 μm. Frit flow rate ($\dot{V}_f$) was adjusted as crossflow rate ($\dot{V}_c$) + $\dot{V}_{out}$ − $\dot{V}_s$. Carrier solution was 0.01 M PBS.

We applied the run conditions indicated in Fig. 1b to analyse human plasma samples treated with different isolation procedures using the FIAF4 channel coupled to UV and MALS detectors in series. Fig. 2a shows the fractograms (both UV and MALS signals at 90°) of the plasma sample treated with ExoLutE® exosome isolation kit at an injection volume of 20 μL. This volume was equivalent to 100 μL of the original serum sample. The volume information provided in the parenthesis of Fig. 2a–c legends represents the amount equivalent to the original serum volume. Although exosome particles were not detected by the UV detector at 280 nm (top panel of Fig. 2a) owing to low concentration, MALS signals at a detection angle of 90° (hereafter MALS-90°) (the lower fractogram of Fig. 2a) could clearly show a broad, but relatively weak signal at 35–50 min that was presumably derived from exosomes. As shown in Fig. 2b and c, the serum sample treated with UC at 120,000×g was injected into FIAF4 channel at different injection volumes. The supernatant liquid after UC was removed, while the obtained pellet was resuspended for the injection to FlFFF. When 100 μL (equivalent to 50 μL of the original serum sample) of the resuspended pellet was injected to FIAF4 channel (Fig. 2b), no signal was

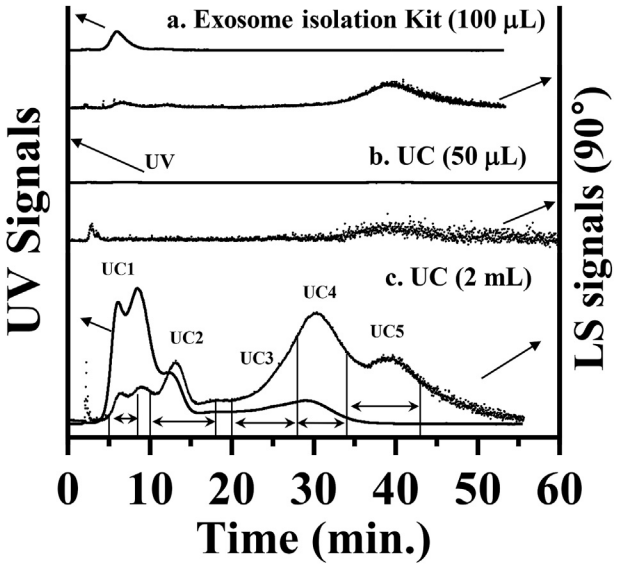

Fig. 2. Comparison of FIAF4 fractograms (UV and MALS-90°) of the serum treated with a) an exosome isolation kit at an injection volume equivalent to 100 μL of the original serum volume and using ultracentrifugation (UC at 120,000×*g*) at an injection volume equivalent to b) 50 μL and c) 2 mL (bottom) of the original serum sample. Run condition of AF4 separation is the same as used in Fig. 1b.

observed from the UV detector, while noisy but weak signals were reported with MALS-90°. As the injection amount was increased to 2 mL of the original serum sample in Fig. 2c, distinct elution profiles were observed with both detectors. Intense peaks (solid line) were detected at 5–15 min, but a relatively weak and broad peak was observed until 35 min by the UV detector. However, MALS detector exhibited relatively smaller peaks at 5–15 min as compared to the intense bimodal peaks reported at 20–55 min. The peaks observed at 5–15 min were probably derived from small particles such as HDL or some proteins that were not completely removed. An opposite trend of UV and MALS-90° signals was observed for smaller species because the UV detector signal is based on the concentration of particles, while MALS detection relies on both concentration and molar mass. Thus, MALS signals for the late eluting large components (20–55 min) were much stronger than the UV signals. During FlFFF runs, five fractions (UC1 to UC5) were collected at the time intervals marked in Fig. 2c to confirm the presence of exosomes using western blotting which will be discussed later. The FlFFF separation of UC-treated samples at different injection amounts revealed that at least 2 mL of the original serum volume was needed to detect exosomes with MALS to allow evaluation of the collected fractions.

The UF-treated serum sample was examined under the run conditions mentioned in Fig. 2. Fig. 3a was obtained after injecting the UF-treated exosome retentate using a 100 kDa membrane at an injection volume of 5 μL, which was equivalent to 50 μL of the original serum sample. Intense UV signals in Fig. 3a were observed between 5 and 15 min, consistent with those reported in Fig. 2c, and were thought to be derived from HDL and few remaining proteins that were not removed by the 100 kDa membrane. However, MALS signals after 35 min were more intense, in line with those observed in Fig. 2c. This observation indicates the increase in the recovery of species with large diameters using UF even at a low injection volume (40-fold less). Detector signals in both Figs. 2 and 3 were plotted at the same scale. The scattered LS signals before 5 min were thought to be derived from smaller sized highly abundant proteins such as albumin or nanometre-sized vesicles that were not completely removed by the membrane concentrator (100 kDa). However, the elution of small molecular weight species at the beginning of FlFFF separation demonstrates that extensive protein removal was not necessary for the isolation of exosome fraction with FlFFF. The same serum sample was subjected to treatment with a 300 kDa membrane concentrator, and the UV signal of the first peak was significantly reduced following the removal of noisy MALS signals at the start of the run (Fig. 3b); however, the peak intensity of the late eluting components after 20 min was not reduced, indicating that UF with 300 kDa membrane did not reduce the population of large diameter vesicles from the retentate. The comparison of the MALS signals for the serum samples treated with three different methods demonstrates that UF with 300 kDa membrane seemed be more efficient at retrieving vesicles with large diameter from the blood serum than UC even with small volumes of samples (equivalent to 50 μL). TEM images of the collected fractions (UF1 to UF5) showed an increase in particle size with an increase in retention time, as is evident from the average radius value measured from each fraction in Table 1. A quantitative comparison of sizes from TEM images was not made herein since exosomes were not fixed with fixative agent and thus, a possibility of morphological change could occur.

3.2. Radii of exosome fractions by MALS and DLS

Root mean square (RMS) radius values were calculated from MALS signals using Zimm (marked with circles) approximation and Sphere (triangles) approximation (Fig. 4a and b) for UC- and UF-treated samples, respectively. Both approximations showed similar size calculation for the eluted components that were smaller than 70 nm in RMS radius. However, the Zimm method yielded much higher results than the Sphere method for particles larger than 70 nm. This observation is in line with the calculated radii of cell-derived exosomes between the two methods, wherein the Zimm RMS method fitted well with the DLS results (hydrodynamic radius, R_h) for smaller particles and the Sphere method approximated well for larger particles [33]. While the Zimm method provided size calculation at a retention time interval of 15–45 min, the sphere method was successful only after 30 min probably due to the low concentrations in early fractions. The hydrodynamic radius values calculated from batch DLS measurements (star symbol) for the fractions collected every 5 min were superimposed with the MALS RMS radius values in Fig. 4a and b. These values can be compared with the fractograms of PS standard particles in Fig. 4c, wherein the particle size was marked with the radius value (half of nominal diameter value). Since the ratio of RMS radius to R_h is 0.775 for hard spheres [36] and 1 for hollow spheres like liposomes [37], it could be useful to compare RMS radius of exosomes with R_h values although exosomes are not perfectly hollow spheres. DLS results obtained using the diameter scale were converted to radius and plotted in Fig. 4a and b. DLS radius values shown in Fig. 4a and b appeared to agree well with the MALS results. The calculated radius values from the batch DLS and MALS radii are compared in Table 2, and the MALS radii in Table 2 were calculated from FlFFF-UV-MALS signals at the specified time interval for each fraction. The comparison of the DLS hydrodynamic radius of each collected fraction with MALS radii (Table 2) showed that Zimm RMS radius values were close to DLS data, the exception being the large size particles, as observed by the steep increase in the calculated radii after 70 nm in both Fig. 4a and b; however, sphere RMS radii calculated at the last two fractions (7 and 8) were similar (less than 4%) to the DLS calculation. We compared the MALS results with the particle sizes of polystyrene standards marked with nominal radius values in Fig. 4b, and found that the Zimm method approximated well with 11, 23, and 51 nm PS particles, while the sphere method fitted well with 102 nm PS particles.

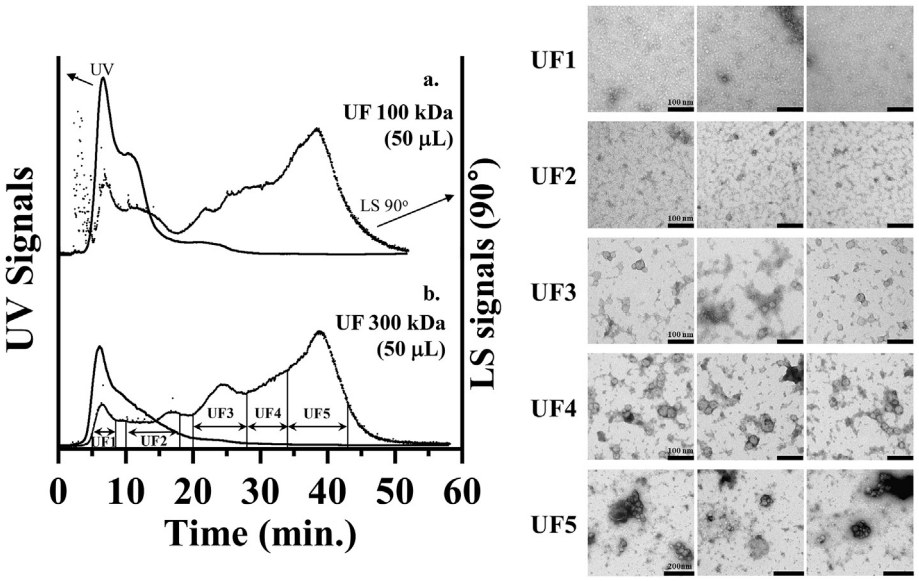

Fig. 3. Fractograms (UV and MALS-90°) of the serum sample after ultrafiltration (UF) using two different membrane filters: 100 kDa for a) and 300 kDa for b). The injection amount was equivalent to 50 μL of the original serum volume. TEM images of the collected fractions are shown.

Table 1
Comparison between the average radius of exosomes measured from TEM images and that calculated from the batch DLS measurement for five collected fractions.

Fraction No.	Time (min)	TEM	
		Average radius (nm)	Count
UF1	5.0–8.5	3.8 ± 1.0	176
UF2	10.0–18.0	5.2. ± 1.4	61
UF3	20.0–28.0	12.7 ± 3.7	34
UF4	28.0–34.0	19.3 ± 6.4	17
UF5	34.0–42.0	48.9 ± 28.4	6

3.3. Western blot analysis of exosome fractions from FlFFF

The collected fractions from both UC- and UF-treated serum samples were analysed by western blotting using antibodies against Alix, CD9, HSP70, and TSG101 that are specific for exosomes (Fig. 5a) and two antibodies against Apo-A and Apo-B for the detection of lipoproteins (Fig. 5b). Alix and TSG101 are endosomal sorting complexes required for transport (ESCRT) proteins that are enriched in exosomes and are involved in multivesicular body biogenesis and exome budding and abscission [38]. While Alix was detected in UC3-UC5 and UF3-UF5 fractions, the two last fractions (UC4 and UC5) showed strong responses to ALIX. Intense signals were detected for UF3 and UF4. These three fractions showed the presence of different populations of exosomes. CD9, a membrane protein, was found in UC4 and UC5 fractions, but the band was more intense in UC5; however, it was detected only in UF3 fraction. As UC was reported to induce a possible increase in the size of exosomes and microvesicles [15], the detection of Alix and CD9 in the last two fractions of the UC-treated sample may be supported by the increase in the size of UC-treated exosomes as compared to that of UF-treated exosomes. However, as UC in general can be effective in retrieving heavier or larger diameter vesicles, there is a possibility of observing large diameter vesicles with UC method. HSP70 is an intracellular heat shock protein that maintains cellular homeostasis, while TSG101 is a member of the ESCRT protein complex that is enriched in exosomes. Both these proteins were found in UC3/UC4 and UF3/UF4 fractions, but were enriched in UC3

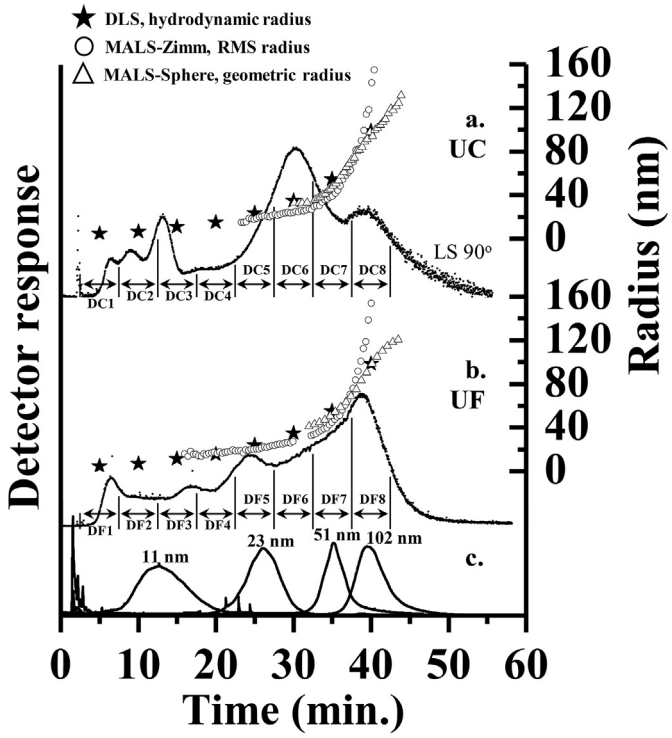

Fig. 4. Plots of radius values calculated from the MALS Zimm method (o), the MALS Sphere method (Δ), and the batch DLS measurement (★) of the eight fractions of a) UC- and b) UF-treated samples along with c) the fractograms (UV) of polystyrene standard beads (11, 23, 51, and 102 nm in radius).

and UF3 fractions. The exosome markers, except Alix, used herein were not detected in UF5, while the MALS-90° signals of the UF5 at 34–42 min (Fig. 3b) appeared to be much greater than those of UC5 (Fig. 2c). This observation supports the possibility that the UF5 fraction may contain some microvesicles despite their removal during the initial centrifugation step. The presence of lipoproteins was confirmed using two antibodies, Apo-A and Apo-B, that are

Table 2
Calculated mean radius (±standard deviation) of exosomes at each time interval based on DLS measurement, the MALS-Zimm method, and the MALS-Sphere method from both UC- and UF-treated serum samples. DLS radius values were Z-average means by the batch DLS measurement of the collected fractions (1–8 for both DC and DF fractions in Fig. 4) and MALS radii were based on MALS signals at time intervals corresponding to each fraction.

Fraction no. (DC/DF)	Time (min)	Radius (nm) - UC			Radius (nm) - UF		
		DLS	MALS-Zimm	MALS-Sphere	DLS	MALS-Zimm	MALS-Sphere
1	2.5–7.5	4.4 ± 2.4	N/C[a]	N/C	4.6 ± 2.3	N/C	N/C
2	7.5–12.5	6.3 ± 4.1	N/C	N/C	6.9 ± 4.1	N/C	N/C
3	12.5–17.5	10.7 ± 6.2	N/C	N/C	11.5 ± 7.2	13.7 ± 2.3[c]	N/C
4	17.5–22.5	14.9 ± 9.2	N/C	N/C	15.3 ± 9.5	16.3 ± 2.1	N/C
5	22.5–27.5	23.5 ± 19.6	18.9 ± 2.0	N/C	23.7 ± 9.8	20.1 ± 1.8	N/C
6	27.5–32.5	34.7 ± 13.8	24.3 ± 2.9	N/C	34.7 ± 23.8	26.2 ± 2.8	N/C
7	32.5–37.5	54.4 ± 30.5	43.2 ± 11.2	55.3 ± 10.7	54.8 ± 29.9	47.0 ± 10.9	53.8 ± 7.8
8	37.5–42.5	98.8 ± 51.7	102.3 ± 27.3[b]	95.2 ± 13.1	98.2 ± 49.7	107.6 ± 24.7[b]	95.8 ± 14.4

[a] Not calculated, Diameter based on data within.
[b] 37.5–40.0 min and.
[c] 15–17.5 min.

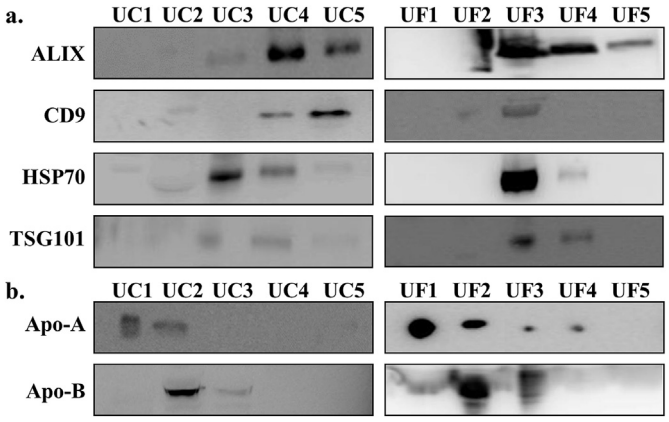

Fig. 5. Western blot results with a) the four exosome markers (ALIX, CD9, HSP70, and TSG101) and b) lipoprotein markers (Apo-A and Apo-B) for the collected fractions of two different exosome preparations: UC- and UF-treated serum samples in Figs. 2 and 3, respectively.

specific for HDL and LDL including VLDL, respectively, (Fig. 5b). UC1/UC2 and UF1/UF2 fractions reacted with Apo-A, indicating that the intense peaks at the start of the separation (Figs. 2c and 3b) originated, at least in part, from the elution of HDL. Moreover, the removal of HDL was more efficient with UC, as is evident from the comparison of the intensities of Apo-A bands between the two samples in Fig. 5b. Apo-B was detected in UC2 and UF2/UF3, with a less intense band in both UC3 and UF3, but was absent in UC4/UC5 and UF4/UF5 fractions. Therefore, UF4 and UF5 fractions were likely to be enriched with exosomes without any lipoprotein contamination. Western blot analysis showed that the UC method is more efficient at removing lipoproteins than the UF method. However, the UF method was more efficient at retrieving exosomes than the UC method even upon the use of small volumes of serum samples (50 μL for UF in comparison to 2 mL for UC). Although the initial centrifugation (10,000×*g*) step in UF was intended to remove cell debris and microvesicles, possible contamination with microvesicles cannot be excluded. Further investigation of this method is warranted.

3.4. Proteomic analysis of exosome fractions

The fractions collected from the two different purification methods were analysed for the identification of proteins. Each fraction was proteolysed using trypsin, and the resulting peptide mixture was subjected to nUHPLC-ESI-MS/MS analysis. A total of 417 and 518 proteins were identified from UC- and UF-treated samples, respectively, with 213 proteins commonly found in both samples. A complete list of the identified proteins in each fraction is shown in Table S1 of Supplementary material. We compared the number of the identified proteins in each fraction between the two methods (Table 3) and found that the number of proteins (156) in UC3 was much lower than that in UF3 (244), whereas the identified number (257) in UC5 was similar to that in UF5 (241). The proteins identified in fractions 3 to 5 in UC and UF fractions were compared with the top 100 exosome proteins found on the exosome protein database, ExoCarta [39], and those that matched with the database are listed in Table 3. While serum albumin and alpha-2-macroglobulin were detected in all fractions except UC5, galectin-3-binding protein, a traditional exosome marker [40], was detected only in the last three fractions derived from both methods (expected to contain exosomes). While the three other proteins (pyruvate kinase, T-complex protein 1 subunit beta, and importin subunit beta-1) were found only in UF5, the two tetraspanin proteins (CD9 and CD81) as well as the Ras-related protein Rap-1b were detected only in UC5. Of these, tetraspanin CD-9, a serum membrane protein, is known to be expressed in exosomes of various sizes as well as in microvesicles [41]. The proteomic analysis of the collected fractions supported the presence of exosomes, but the number of exosome proteins found in UC3-UC5 and UF3-UF5 was relatively small owing to the small injection volumes of the samples in FlFFF. Nonetheless, it was indicated that exosomes can be size-sorted and isolated from LDL particles using field programmed separation of FlFFF.

4. Conclusions

In this study, FlFFF-MALS was employed to investigate the performance of exosome isolation from human serum using an exosome isolation kit, UC and UF methods; the collected fractions were confirmed with western blotting and proteomic analysis using nUHPLC-ESI-MS/MS. A simple centrifugation followed by UF with membrane filter units (300 kDa pores) offered advantages such as faster preparation and higher exosomal recovery with small sample volumes (50 μL) than the UC method (2 mL at least). However, the removal of lipoproteins seemed more efficient with UC than with UF. Although the serum contains numerous proteins, lipoproteins, exosomes, and microvesicles, here we demonstrate the application of FlFFF with a programmed decay of the crossflow rate for the isolation of most exosomes from HDL and LDL. VLDLs that are present at relatively lower levels in the serum compared to other lipoproteins were not completely removed from the smaller sized exosomes owing to their size similarity. It is imperative to develop a

Table 3
List of exosome proteins in each fraction (UF and UC fractions) after comparison with the ExoCarta database.

Fractions	UC1/UF1	UC2/UF2	UC3/UF3	UC4/UF4	UC5/UF5
Number of proteins	71/88	164/203	156/244	172/194	257/241
Commonly found	46	96	92	100	145
Proteins from ExoCarta					
Serum albumin	O/O	O/O	O/O	O/O	/O
Alpha-2-macroglobulin	O/O	O/O	O/O	O/O	O/O
Galectin-3-binding protein			O/O	O/O	O/O
Thrombospondin-1				/O	O/O
Pyruvate kinase					/O
T-complex protein 1 subunit beta					/O
Importin subunit beta-1					/O
Transferrin receptor (P90, CD71), isoform CRA_c		O/			O/
Tetraspanin CD9					O/
Tetraspanin CD81					O/
Ras-related protein Rap-1b					O/

highly efficient method to deplete VLDL from serum samples prior to FlFFF separation without incorporating any affinity column-based method, which may deform or trap extracellular vesicles during passage. However, the present study shows that the UF protocol with FlFFF-MALS may be used as an isolation method to retrieve exosomes once a preparative scale FlFFF channel such as a multilane channel system to increase throughput is implemented. Moreover, centrifugation steps during the preliminary exclusion of cell debris and microvesicles may be further optimised to retrieve exosomes and microvesicles in series using FlFFF-MALS.

Funding

This study was supported by the grant (NRF-2018R1A2A1A05019794) of the Ministry of Science, ICT & Future Planning through the National Research Foundation (NRF) of Korea.

Declaration of competing interest

The authors declare that they have no known competing financial interests or personal relationships that could have appeared to influence the work reported in this paper.

CRediT authorship contribution statement

Young Beom Kim: Investigation, Methodology, Writing - original draft. **Joon Seon Yang:** Data curation. **Gwang Bin Lee:** Formal analysis. **Myeong Hee Moon:** Supervision, Writing - review & editing.

Appendix A. Supplementary data

Supplementary data to this article can be found online at https://doi.org/10.1016/j.aca.2020.05.031.

References

[1] K. Denzer, M.J. Kleijmeer, H.F. Heijnen, W. Stoorvogel, H.J. Geuze, Exosome: from internal vesicle of the multivesicular body to intercellular signaling device, J. Cell Sci. 113 Pt 19 (2000) 3365–3374.
[2] R.M. Johnstone, M. Adam, J.R. Hammond, L. Orr, C. Turbide, Vesicle formation during reticulocyte maturation. Association of plasma membrane activities with released vesicles (exosomes), J. Biol. Chem. 262 (1987) 9412–9420.
[3] C. Thery, L. Zitvogel, S. Amigorena, Exosomes: composition, biogenesis and function, Nat. Rev. Immunol. 2 (2002) 569–579.
[4] E.R. Sauter, Exosomes in blood and cancer, Transl. Canc. Res. 6 (2017) S1316–S1320.
[5] P. Vader, X.O. Breakefield, M.J.A. Wood, Extracellular vesicles: emerging targets for cancer therapy, Trends Mol. Med. 20 (2014) 385–393.
[6] G. Raposo, W. Stoorvogel, Extracellular vesicles: exosomes, microvesicles, and friends, J. Cell Biol. 200 (2013) 373–383.
[7] E. Hosseini-Beheshti, S. Pham, H. Adomat, N. Li, E.S.T.J.M. Guns, c. proteomics, Exosomes as biomarker enriched microvesicles: characterization of exosomal proteins derived from a panel of prostate cell lines with distinct, AR Phenotypes 11 (2012) 863–885.
[8] T. Baranyai, K. Herczeg, Z. Onódi, I. Voszka, K. Módos, N. Marton, G. Nagy, I. Mäger, M.J. Wood, S.J.P.o. El Andaloussi, Isolation of Exosomes from Blood Plasma: Qualitative and Quantitative Comparison of Ultracentrifugation and Size Exclusion Chromatography Methods, vol. 10, 2015, e0145686.
[9] A.N. Böing, E. Van Der Pol, A.E. Grootemaat, F.A. Coumans, A. Sturk, R. Nieuwland, Single-step isolation of extracellular vesicles by size-exclusion chromatography, J. Extracel. Vesicles 3 (2014) 23430.
[10] Y. Weng, Z. Sui, Y. Shan, Y. Hu, Y. Chen, L. Zhang, Y.J.A. Zhang, Effective isolation of exosomes with polyethylene glycol from cell culture supernatant for in-depth proteome profiling 141 (2016) 4640–4646.
[11] D.W. Greening, R. Xu, H. Ji, B.J. Tauro, R.J. Simpson, A Protocol for Exosome Isolation and Characterization: Evaluation of Ultracentrifugation, Density-Gradient Separation, and Immunoaffinity Capture Methods, Proteomic Profiling (2015) 179–209.
[12] B.J. Tauro, D.W. Greening, R.A. Mathias, H. Ji, S. Mathivanan, A.M. Scott, R.J. Simpson, Comparison of ultracentrifugation, density gradient separation, and immunoaffinity capture methods for isolating human colon cancer cell line LIM1863-derived exosomes, Methods 56 (2012) 293–304.
[13] H. Kalra, C.G. Adda, M. Liem, C.S. Ang, A. Mechler, R.J. Simpson, M.D. Hulett, S.J.P. Mathivanan, Comparative proteomics evaluation of plasma exosome isolation techniques and assessment of the stability of exosomes in normal human blood plasma vol. 13 (2013) 3354–3364.
[14] E. Zeringer, T. Barta, M. Li, A.V. Vlassov, Strategies for isolation of exosomes, Cold Spring Harb. Protocols (2015) 319–323.
[15] F. Momen-Heravi, L. Balaj, S. Alian, A.J. Trachtenberg, F.H. Hochberg, J. Skog, W.P. Kuo, Impact of biofluid viscosity on size and sedimentation efficiency of the isolated microvesicles, Front. Physiol. vol. 3 (2012) 162.
[16] C. Théry, S. Amigorena, G. Raposo, A. Clayton, Isolation and characterization of exosomes from cell culture supernatants and biological fluids, Curr. Protocols Cell Biol. (2006) chapter 3, 3.22.
[17] Y. Yuana, J. Levels, A. Grootemaat, A. Sturk, R. Nieuwland, Co-isolation of extracellular vesicles and high-density lipoproteins using density gradient ultracentrifugation, J. Extracell. Vesicles 3 (2014).
[18] B.W. Sodar, A. Kittel, K. Paloczi, K.V. Vukman, X. Osteikoetxea, K. Szabo-Taylor, A. Nemeth, B. Sperlagh, T. Baranyai, Z. Giricz, Z. Wiener, L. Turiak, L. Drahos, E. Pallinger, K. Vekey, P. Ferdinandy, A. Falus, E.I. Buzas, Low-density lipoprotein mimics blood plasma-derived exosomes and microvesicles during isolation and detection, Sci. Rep. 6 (2016) 24316.
[19] N. Karimi, A. Cvjetkovic, S.C. Jang, R. Crescitelli, M.A.H. Feizi, R. Nieuwland, J. Lötvall, C.J.C. Lässer, m.I. sciences, Detailed analysis of the plasma extracellular vesicle proteome after separation from lipoproteins 75 (2018) 2873–2886.
[20] T. Wang, I.V. Turko, Proteomic toolbox to standardize the separation of extracellular vesicles and lipoprotein particles, J. Proteome Res. vol. 17 (2018) 3104–3113.
[21] J.C. Giddings, Field-flow fractionation: analysis of macromolecular, colloidal, and particulate materials, Science 260 (1993) 1456–1465.
[22] B. Roda, A. Zattoni, P. Reschiglian, M.H. Moon, M. Mirasoli, E. Michelini, A. Roda, Field-flow fractionation in bioanalysis: a review of recent trends, Anal. Chim. Acta 635 (2009) 132–143.
[23] M.H. Moon, Flow field-flow fractionation: recent applications for lipidomic and proteomic analysis, Trac. Trends Anal. Chem. 118 (2019) 19–28.
[24] J.C. Giddings, Field flow fractionation - a versatile method for the characterization of macromolecular and particulate materials, Anal. Chem. 53 (1981)

1170–&.
[25] M. Nilsson, L. Bulow, K.G. Wahlund, Use of flow field-flow fractionation for the rapid quantitation of ribosome and ribosomal subunits in Escherichia coli at different protein production conditions, Biotechnol. Bioeng. 54 (1997) 461–467.
[26] L.F. Pease 3rd, D.I. Lipin, D.H. Tsai, M.R. Zachariah, L.H. Lua, M.J. Tarlov, A.P. Middelberg, Quantitative characterization of virus-like particles by asymmetrical flow field flow fractionation, electrospray differential mobility analysis, and transmission electron microscopy, Biotechnol. Bioeng. 102 (2009) 845–855.
[27] I. Park, K.J. Paeng, Y. Yoon, J.H. Song, M.H. Moon, Separation and selective detection of lipoprotein particles of patients with coronary artery disease by frit-inlet asymmetrical flow field-flow fractionation, J Chromatogr B Analyt Technol Biomed Life Sci 780 (2002) 415–422.
[28] D.C. Rambaldi, P. Reschiglian, A. Zattoni, C. Johann, Enzymatic determination of cholesterol and triglycerides in serum lipoprotein profiles by asymmetrical flow field-flow fractionation with on-line, dual detection, Anal. Chim. Acta 654 (2009) 64–70.
[29] J.S. Yang, J.Y. Lee, M.H. Moon, High speed size sorting of subcellular organelles by flow field-flow fractionation, Anal. Chem. 87 (2015) 6342–6348.
[30] H. Lee, S.K. Williams, K.L. Wahl, N.B. Valentine, Analysis of whole bacterial cells by flow field-flow fractionation and matrix-assisted laser desorption/ionization time-of-flight mass spectrometry, Anal. Chem. 75 (2003) 2746–2752.
[31] P. Reschiglian, A. Zattoni, B. Roda, L. Cinque, D. Melucci, B.R. Min, M.H. Moon, Hyperlayer hollow-fiber flow field-flow fractionation of cells, J. Chromatogr. A 985 (2003) 519–529.
[32] J.S. Yang, J.C. Lee, S.K. Byeon, K.H. Rha, M.H. Moon, Size dependent lipidomic analysis of urinary exosomes from patients with prostate cancer by flow field-flow fractionation and nanoflow liquid chromatography-tandem mass spectrometry, Anal. Chem. 89 (2017) 2488–2496.
[33] K.E. Petersen, E. Manangon, J.L. Hood, S.A. Wickline, D.P. Fernandez, W.P. Johnson, B.K. Gale, A review of exosome separation techniques and characterization of B16-F10 mouse melanoma exosomes with AF4-UV-MALS-DLS-TEM, Anal. Bioanal. Chem. 406 (2014) 7855–7866.
[34] J.S. Yang, J.Y. Kim, J.C. Lee, M.H. Moon, Investigation of lipidomic perturbations in oxidatively stressed subcellular organelles and exosomes by asymmetrical flow field-flow fractionation and nanoflow ultrahigh performance liquid chromatography-tandem mass spectrometry, Anal. Chim. Acta 1073 (2019) 79–89.
[35] J.S. Yang, J. Qiao, J.Y. Kim, L. Zhao, L. Qi, M.H. Moon, Online proteolysis and glycopeptide enrichment with thermoresponsive porous polymer membrane reactors for nanoflow liquid chromatography-tandem mass spectrometry, Anal. Chem. 90 (2018) 3124–3131.
[36] W. Vandesande, A. Persoons, The size and shape of macromolecular structures - determination of the radius, the length, and the persistence length of rodlike micelles of dodecyldimethylammonium chloride and bromide, J Phys Chem-Us 89 (1985) 404–406.
[37] O. Stauch, R. Schubert, G. Savin, W. Burchard, Structure of artificial cytoskeleton containing liposomes in aqueous solution studied by static and dynamic light scattering, Biomacromolecules 3 (2002) 565–578.
[38] D.D. Taylor, C. Gercel-Taylor, Exosomes/microvesicles: Mediators of Cancer-Associated Immunosuppressive Microenvironments, Seminars in Immunopathology, Springer, 2011, pp. 441–454.
[39] S. Mathivanan, R.J.J.P. Simpson, ExoCarta: A compendium of exosomal proteins and RNA 9 (2009) 4997–5000.
[40] C. Escrevente, N. Grammel, S. Kandzia, J. Zeiser, E.M. Tranfield, H.S. Conradt, J.J.P.o. Costa, Sialoglycoproteins and N-Glycans from Secreted Exosomes of Ovarian Carcinoma Cells, vol. 8, 2013, e78631.
[41] A. Bobrie, M. Colombo, S. Krumeich, G. Raposo, C. Théry, Diverse subpopulations of vesicles secreted by different intracellular mechanisms are present in exosome preparations obtained by differential ultracentrifugation, J. Extracell. Vesicles 1 (2012) 18397.